# Performance of Rate Splitting Multiple Access-based Visible Light Communications with Residual Interference and Channel Estimation Errors

Sundaresan Sabapathy, *Graduate Student Member, IEEE*, and Surendar Maruthu, *Member, IEEE*

Original scientific article

***Abstract*—Rate splitting multiple access (RSMA) is a powerful and upcoming multiple access technique that can serve as a promising technology for 5G and beyond applications. Due to the increase in the number of indoor communication devices, the internet of everything (IoE) demands higher bandwidth. Visible light communication (VLC) would be a viable solution for an indoor environment that offers high bandwidth, cost-free spectrum, and low power, and if employed with RSMA, the sum rate can be maximized. In this paper, we derive the closed-form outage probability (OP) for the downlink RSMA-based VLC scheme over Rayleigh and Rician channels. We perform outage analyses for perfect as well as imperfect channel state information (CSI) and successive interference cancellation (SIC), respectively to study the system characteristics. Also, we show the superiority of RSMA over non-orthogonal multiple access (NOMA) for VLC-based system in terms of OP over Rayleigh and Rician channels. From the simulations, we show that the RSMA-based VLC system outperforms conventional NOMA-based VLC and the quality of services improves with the line of sight communication i.e., the Rician fading channel.**

***Index Terms*—Rate splitting multiple access, Outage, Visible light communications, Rayleigh channel, Rician Channel.**

## I. Introduction

Over the past few years, the need for seamless connectivity and enhanced data rate has been increasing rapidly. To cope with this everlasting demand, various novel schemes and techniques are put forth day-to-day. Rate splitting multiple access (RSMA) is one such recent technology that has the flexibility to solve connectivity demand and is the front-runner for the upcoming 6G. RSMA can efficiently reduce system complexity and aid in improving the quality of services (QoS) [1]–[3]. Nevertheless, visible light communications (VLC) have extraordinary features such as huge bandwidth, high frequency, and a wider unlicensed spectrum. It consists of low-power transmitters and receivers which serve as the perfect substitute for the ever-upgrading mobile communication technologies [4]. VLC utilizes frequencies ranging from $4.3 \times 10^{14} Hz$ to $7.5 \times 10^{14} Hz$ in the electromagnetic spectrum. The basic principle of VLC is that the signals are intensity modulated (IM) and information is transmitted through the light-emitting diode (LED) at the transmitter end over a wireless channel. At the receiver, the photo detector (PD) is utilized for demodulation [5]. The VLC-based system works efficiently when there is an unobstructed line-of-sight (LOS) path between the transmitter and receiver, whereas, with the presence of obstacles desired performance may not be achieved [4], [5]. Conventionally, outdoor as well as indoor wireless communication system exploits radio frequencies (RF) for the transmission of data, and obtaining the license of the frequency spectrum contributes to more than $50\%$ of the budget estimation. Various room geometrics have been tested over RF and VLC to understand the flexibility of VLC to be used in the future, especially for area spectral efficiency (ASE). Results have shown that ASE gain of VLC-based communication has been dominated over RF-based communication and the VLC system also enhances the data rate of end users [6]. The fundamental analysis on VLC channel over multipath fading (reflection and interference) is modeled numerically in [7]. The key analysis is on field of view, date rate and the received signal power with inter symbol interference tracking technique. The simulation results show that VLC is a strong candidate for future wireless communication systems. Moreover, the capability of VLC with laser source offering high capacity and the channel gain is analyzed in [8] for enacting the stability of VLC system. To enhance the data rate and signal-to-interference plus noise ratio (SINR) for indoor VLC-based systems, diversity combining techniques are adopted in [9]. Moreover, the potentials of VLC-based communication are explored in [10] which proves it to be a promising technology in 6G with terahertz bandwidth. Another platform where VLC plays an important role is vehicle-to-everything (V2X) communications which are experimented in [11]. The analyses were carried out at various environmental constraints with on-off keying modulation and showed that VLC supports enhancing the data rate and SINR.

Likewise, in [12] VLC is adopted for outdoor bidirectional vehicle-to-vehicle communication, and analyses in terms of SINR and packet error rate (PER) are carried out. Results prove that VLC enhances the QoS and offers cost-efficient V2V communication even in outdoor environments. Further, to estimate the dynamic channel and its behavior in VLC, the variants of least mean square techniques are adopted in [13]. The VLC system is analyzed under high and low density users, which requires adaptive algorithms for estimation and

Manuscript received February 7, 2024; revised March 4, 2024. Date of publication May 17, 2024. Date of current version May 17, 2024. The associate editor prof. Tianhua Xu has been coordinating the review of this manuscript and approved it for publication.

Authors are with the Department of Electronics and Communication Engineering, National Institute of Technology Puducherry, Karaikal-609609, India (e-mails: sundaresanece91@gmail.com, surendar.m@nitpy.ac.in).

Digital Object Identifier (DOI): 10.24138/jcomss-2024-0013

depicts that VLC offers better quality of services. Also in [14], VLC is investigated with non-orthogonal multiple access (NOMA)-based transmission for the internet of things (IoT) applications to achieve massive connectivity. The key contribution lies in fair power allocation (FPA) to users and the study proves that the NOMA-based VLC system is superior to conventional NOMA technique in terms of data rate, sum rate, system fairness, energy efficiency, bit error rate, and computational complexity. Additionally, VLC is examined with a partial data-carrying subcarrier (PDS) precoding scheme [15] for combating frequency selective fading and enhancing the SINR in the intelligent transportation system. Furthermore, VLC is analyzed with a relay-based NOMA scheme in [16] and conferred that system is less outage despite information transmission with lower power. The potential of hybrid communication scenario viz., RF/VLC system is analyzed for determining its outage for IoT applications in [17]. Also, the energy harvesting capability of the hybrid system is exploited for optimal harvesting time with various optical parameters. Likewise, in [18] the outage probability and the robustness of the hybrid system viz., free space optics and VLC is aided for outdoor and indoor environment, respectively. The simulation results show that transmit power and channel characteristics decides the performance of the system.

Nonetheless, RSMA analysis proves that enhancing the QoS in the unicast and multicast transmission systems were found to be efficient with less complexity [19]. Moreover, imperfect successive interference cancellation (ISIC) and imperfect channel state information (ICSI) analysis is much needed to study the characteristics of a wireless system in a practical scenario. In [20], the potential of RSMA in the multi-antenna system is exploited and achievable rates by common and private parts are obtained. Also, precoder optimization is performed to enhance the system performance with less complexity at the decoding end. Further, practical implementation is realized through ICSI analysis and shows that the proposed model outperforms conventional decoding schemes. Also, RSMA in the uplink scenario is analyzed in terms of outage and throughput for random access IoT networks [21]. Firstly, the closed form expression for the outage is derived over a Rayleigh fading channel and subsequently the final outage expression is aided for obtaining the throughput of the system. It is shown that RSMA-based system outperforms conventional techniques and aids in increasing the coverage. Further, RSMA outage performance with millimeter wave (mmWave) is exploited in [22] over the correlated fading channel with sparse and multipath scattering. The outage analyses are carried out with two beam-forming techniques viz., transmit common messages on the common paths (TCCP) and transmit common messages on all the paths (TCAP) to enhance the reliability of RSMA. Also, the asymptotic outage is derived for understanding deeper insights into the performance of the system. In [23], the outage and ergodic rate performance of RSMA-based cognitive radio networks is studied for enhancing reliability. The ISIC and ICSI constraints are also considered to analyze the system under practical scenarios. To enhance the sum rate, RSMA with the semi-grant-free transmission is explored in [24] without worsening the outage of the system. Joint optimization of key parameters with shared grant resource blocks and analysis of outage for target data rate and the number of grant-free users is carried out. Likewise, sum rate optimization with ICSI is analyzed for the RSMA system in [25]. Results prove that RSMA is robust to the ICSI and enhances the QoS.

RSMA integrated with VLC enhances energy efficiency (EE), data rate, and massive coverage when compared to traditional techniques such as NOMA and space division multiple access (SDMA). RSMA provides flexibility over conventional multiple access techniques and can be easily adapted to enhance the QoS [26]–[30]. In [26] and [27], RSMA-based VLC is exploited for sum rate maximization and spectral efficiency over NOMA and conferred that RSMA with VLC performs better. Likewise, performance enhancement in terms of energy efficiency and user mobility is observed in RSMA-based VLC analysis with coordinated beam-forming techniques for the private and common parts of RSMA [28]–[30]. We note that in the literature majority of the works with RSMA and VLC are focused on sum rate maximization, bit error rate (BER), symbol error rate (SER), and beam-forming techniques. To the best of the author's knowledge, performance analysis for outage probability (OP) with ISIC and ICSI factors has not been reported, so far. This is the first work to analyze RSMA-based VLC communication in terms of system outage in the presence of ICSI and ISIC. The RSMA-based VLC system is exploited over the LOS and non-LOS (NLOS) propagation viz., Rician and Rayleigh probability density functions (PDF) for obtaining the closed form expressions of the system outage.

The major contributions of this paper are:

- Closed-form OP expressions are derived with the help of SINR over Rayleigh and Rician distribution considering the VLC parameters.
- OP analyses is performed for various threshold rate and also the impact of ICSI and ISIC is been studied. Four combinations of perfect and imperfect scenarios viz.,
    1) Perfect CSI (PCSI) and Perfect SIC (PSIC).
    2) ICSI and PSIC.
    3) PCSI and ISIC.
    4) ICSI and ISIC over Rayleigh and Rician distribution channels are investigated.
- We validate the analytical results obtained from each case with Monte Carlo (MC) simulations for RSMA-based VLC communication system.
- Also, the outage performance of RSMA-based VLC system is compared with NOMA over various transmit signal-to-noise ratio (SNR) and inferred that the former outperforms the latter.

The rest of the paper is organized as follows. Section II explains the system model considered for RSMA-based VLC communication with its mathematical equations. Section III and section IV derive the closed-form outage expressions over Rayleigh and Rician channels with all the possible combinations of perfect and imperfect CSI and SIC, respectively. In section V, analytical expressions are validated through

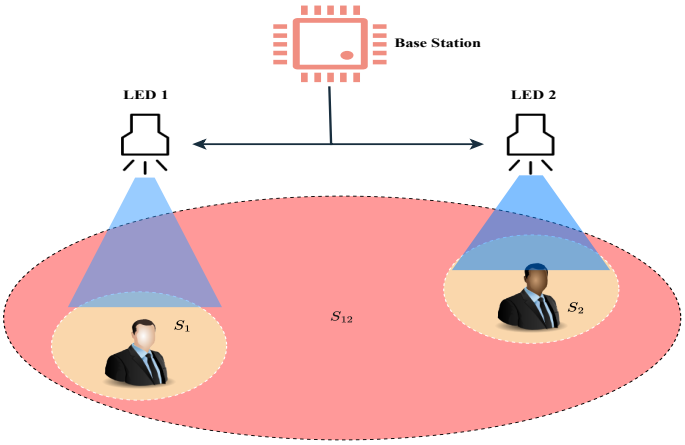


Fig. 1. System model for RSMA with VLC.

MC simulations and each of the analyses is discussed. The conclusions are gathered in section VI.

## II. System Model and Mathematical Background

A simple downlink single-cell two-user scenario aided by RSMA with VLC for transmission and reception of information has been sketched in Figure 1 (for ease of understanding). Without loss of generality, the system can be extended to $K$ users and $L$ cells with multiple users within each cell. In RSMA, the information of each user is separated into common and private parts followed by multiplexing to harvest the benefits of rate splitting and attain enhanced performance. The segregation of common part and private part from each user is based on the channel state information at the transmitter i.e, weak user contributes maximum for the common part. Subsequently, the common part of each user is combined to form the common data (CD) and rest of the information from each user is the private data. Eventually, multiplexed common data and private data are precoded and transmitted over the channel with the help of an LED that has faster switching rates. On the receiver side, PDs are aided to decode the common part which has high power, and private parts are decoded separately by each user assuming the other user's private part as noise through SIC. Moreover, the number of SIC layers is low compared to the NOMA technique due to precoding and partially decoding the interference and partially treating interference as noise.

The system with $K$ number of users and $N_t \times N_r$ LEDs and PDs at the transmitter and receiver end respectively is sketched as block diagram in Figure 2. For ease of understanding and analytical simplicity, we consider two users at the receiver end. At the transmitter end, user 1 and user 2 messages $(M_1, M_2)$ are split into private $(M_1^1, M_2^2)$ and common parts $(M_1^{12}, M_2^{12})$. Now, both the user's common parts are multiplexed together and the private part of each user is encoded individually forming the streams $S_{12}$ and $S_1, S_2$ respectively. Furthermore, the encoded streams are precoded i.e., multiplying $S_{12}, S_1$, and $S_2$ by weights (precoder matrices). Precoding is essential to wisely detect the signal and reduce interference at the receiver end. Finally, the precoded data is transmitted via LED with IM over the wireless fading channel and the characteristics of LED and PD plays a vital role in deciding the QoS.

Let the transmitted stream of a vector be denoted as $\mathbf{S} = [\mathbf{S_1}, \mathbf{S_2}, \mathbf{S_{12}}]^T$, the precoder matrix to reduce interference be $\mathbf{P} = [\mathbf{P_1}, \mathbf{P_2}, \mathbf{P_{12}}]$, and $\mathbf{I}_{DC}$ is to make sure that input to the LED is always positive. The terms $\mathbf{I}_{DC} \in [\mathbf{I}_L, \mathbf{I}_H]$ where $\mathbf{I}_L$ and $\mathbf{I}_H$ are the minimum and maximum DC bias offset in LED linear region respectively. The imposed transmitted signal can be defined mathematically as,

$$\mathbf{x} = \sum_{i \in (1,2,12)} (\mathbf{P}_i \mathbf{S}_i) + \mathbf{I}_{DC}. \tag{1}$$

Now, the received signal at $k$-th PD is expressed as,

$$\mathbf{y}_k = \xi \zeta \mathbf{h}_k^T \mathbf{x} + \mathbf{n}_k, \forall k \in \{1, 2\}, \tag{2}$$

where, $\xi$ represents the LED conversion factor and $\zeta$ is the photo detector responsivity, $\mathbf{h}_k^T = [\mathbf{h}_{k,1}, \mathbf{h}_{k,2}]^T$ is the channel vector between transmitter LED and receiver PD and $\mathbf{n}_k$ is the Gaussian noise. After passing through a wireless channel, the transmitted signals are detected by PD at each user separately through direct detection (DD). The channel gain ($\mathbf{h}$) is modeled in terms of Lambertian emission pattern [31] and can be mathematically expressed as,

$$\mathbf{h}_k = \frac{(m+1) A_k \zeta cos\varpi}{2\pi d_k^2} cos^m(\theta) g(\varpi) \tau(\varpi), \tag{3}$$

where, $m$ is the Lambertian emission order, $\varpi$ and $\theta$ are the incident and radiation angle respectively, $g(\varpi) = \frac{n^2}{sin^2(\psi)}, 0 \leq \varpi \leq \psi$ is the optical concentrator gain which depends on refractive index and field of view of photo detector, $A_k$ is the detection area of the PD, $d_k$ is the Euclidean distance and $\tau(\varpi)$ is the optical filter gain. This channel coefficient is utilized for calculating the SINR of RSMA-based VLC system. At the receiver, the common part is initially decoded and SIC is performed to the left-out signal to decode the intended user private part which is combined with common part to form the original message. The decoding order at the receiver is common part followed by the private part of the other user and finally the private part of the intended user through SIC. To be precise, firstly the common part $S_{12}$ is decoded treating private parts of the intended user and other users as noise, and its corresponding SINR at $k$th user can be mathematically written in terms of Lambertian emission as,

$$\gamma_k^{12} = \frac{\rho \left| \mathbf{h}_k^T \mathbf{P}_{12} \right|^2}{\rho \left| \mathbf{h}_k^T (\mathbf{P}_1^2 + \mathbf{P}_2^2) \right|^2 + 1} \tag{4}$$

where, $\rho = \frac{(\xi\zeta)^2}{\sigma^2}$ is the transmission SNR. For ease of calculations, we assume $\xi, \zeta$ are unity. After decoding the common parts, it is removed from the original received message through SIC and the remaining signal will be the private parts of the intended user and the other user. Now, the receiver decodes the intended private part by treating the other user private part as noise, and its corresponding SINR is defined as,

$$\gamma_k^{\mathcal{K}} = \frac{\rho \left| \mathbf{h}_k^T \mathbf{P}_k \right|^2}{\rho \left| \mathbf{h}_k^T \mathbf{P}_{\mathcal{K}} \right|^2 + 1} \quad ; \quad (k, \mathcal{K}) \in \{(1,2), (2,1)\} \tag{5}$$

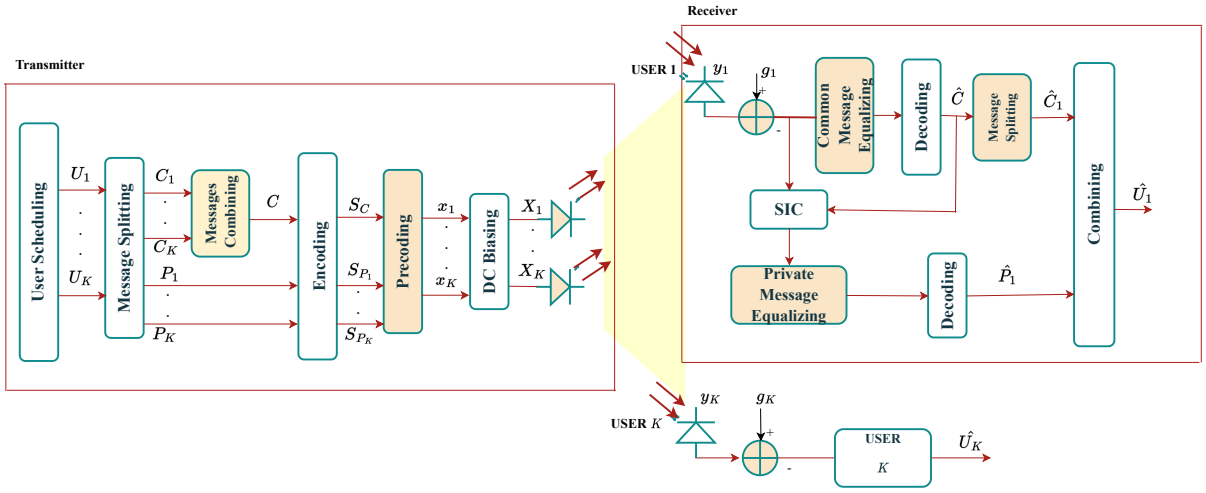


Fig. 2. Block diagram for downlink RSMA with VLC for $K$ users.

The condition for maximum allowable rate of common part and private part at which information can be transmitted successfully at $k$-th PD is mathematically written as,

$$\begin{aligned} R_k^{12} &= log_2\left(1+\gamma_k^{12}\right) \geq R1, \\ R_k^{\mathcal{K}} &= log_2\left(1+\gamma_k^{\mathcal{K}}\right) \geq R2 \quad for\ k,\mathcal{K} \in (1,2)\,. \end{aligned} \tag{6}$$

The terms $R_k^{12}$ and $R_k^{\mathcal{K}}$ represents the respective user common and private part bit rates and $R1,\ R2$ represents the target bit rates of common and private parts. Thus, the overall bit rate of the RSMA system is described as,

$$R_k\ = R_{k,\ common}\ +\ R_k^{\mathcal{K}} \quad for\ k,\mathcal{K} \in (1,2)\,, \tag{7}$$

where, $R_{k,\ common}$ is the $k$-th user portion of the total common rate. The OP analysis of RSMA-based VLC system is carried out over LOS and NLOS paths with perfect and imperfect CSI and SIC for studying the system behavior under ideal and realistic scenario in the next section.

## III. Outage Analyses Over Rayleigh Fading Channel

A system is said to be in outage if the rate at which information is being transmitted is less than the threshold (target) information rate [32]. In RSMA-based VLC, the system is in outage if either the common part or private part is outage. Moreover, the common part is transmitted with high power and its outage forces the private part also to be in outage. The condition for the common part to be in outage is expressed as,

$$R_k^{12} = log_2\left(1+\left[\frac{\rho\gamma_k\left(\mathbf{P}_k\right)^2}{\rho\gamma_k\left(\mathbf{P}_{\mathcal{K}}\right)^2+1}\right]\right) < R1\,(k,\mathcal{K}) \in \{(1,2),(2,1)\}\,. \tag{8}$$

For ease of calculations, we assume the channel coefficient $|\mathbf{h}_k^T|^2 = \gamma_k$, and $\gamma_t$ is the target SNR such that the outage expression is given by,

$$\gamma_k^{12} < \gamma_t. \tag{9}$$

The threshold condition for two user scenario with channel coefficient is described as,

$$\gamma_1 < \frac{\gamma_t}{\rho\left[\mathbf{P}_{12}^2 - \gamma_t\left(\mathbf{P}_1^2+\mathbf{P}_2^2\right)\right]} \Rightarrow \gamma_{th}, \tag{10}$$

where $\gamma_{th}$ is the minimum threshold value. In this section, Rayleigh distribution is exploited for RSMA-based VLC, wherein, it describes the received signal amplitude due to factors such as reflections, scattering, and interference in the optical wireless communication channel. To be precise, the Rayleigh distribution is commonly used in indoor environments where there can be various obstacles and reflective surfaces and aids in modeling the amplitude of the received signal when there is no dominant LOS between the transmitter and receiver [33], [34]. It accurately describes the fading characteristics caused by multipath propagation, where the signal reaches the receiver through multiple indirect paths and its corresponding PDF is given by,

$$f_\gamma\left(\gamma\right) = \left(\frac{1}{\bar{\gamma}}\right)^2 e^{\frac{-\gamma}{(\bar{\gamma})^2}}. \tag{11}$$

where $\gamma$ is the random variable and $\bar{\gamma}$ is the mean of that random variable i.e., $E[\gamma] = \bar{\gamma}$. The OP for the common part alone over Rayleigh distribution can be expressed mathematically as,

$$P_{out,\ common} = \int_0^{\gamma_{th}} f_\gamma\left(\gamma\right) d\gamma. \tag{12}$$

The closed form outage for the common part is calculated by integrating (10) with respect to $\gamma$ from $\gamma_{th}$ to $\infty$ and the expression is given by,

$$P_{out,\ common} = 1 - exp\left[\frac{-\gamma_t}{(\bar{\gamma})^2\,\rho\left[\mathbf{P}_{12}^2 - \gamma_t\left(\mathbf{P}_1^2+\mathbf{P}_2^2\right)\right]}\right]. \tag{13}$$

Likewise, the condition for the private part to be in outage is described as,

$$R_k^{\mathcal{K}} = log_2\left(1+\frac{\rho\left|\mathbf{h}_k^T\mathbf{P}_k\right|^2}{\rho\left|\mathbf{h}_k^T\ \mathbf{P}_{\mathcal{K}}\right|^2+1}\right) < R2, \forall\ (k,\ \mathcal{K}) \in \{(1,2),(2,1)\}\,. \tag{14}$$

The outage at the private part also depends on whether the common part gets outage or not i.e., if the common part is in outage, then the private part will also be in outage. So, the threshold SINR is expressed as,

$$\gamma_{th} = \max\left\{ \frac{\gamma_t}{\rho\left[\mathbf{P}_k^2 - \gamma_t \mathbf{P}_{\mathcal{K}}^2\right]} \;\;,\;\; \frac{\gamma_t}{\rho\left[\mathbf{P}_{12}^2 - \gamma_t\left(\mathbf{P}_1^2 + \mathbf{P}_2^2\right)\right]} \right\}. \quad (15)$$

Now, the OP of the private part can be evaluated by integrating the PDF of the Rayleigh fading channel in (12) with respect to $\gamma$ from $\gamma_{th}$ to $\infty$ in (15). Its corresponding closed-form expression is obtained as,

$$P_{\text{out, private}} = 1 - \exp\left[ -\frac{1}{(\bar{\gamma})^2} \max\left\{ \frac{\gamma_t}{\rho\left[\mathbf{P}_k^2 - \gamma_t \mathbf{P}_{\mathcal{K}}^2\right]}, \frac{\gamma_t}{\rho\left[\mathbf{P}_{12}^2 - \gamma_t\left(\mathbf{P}_1^2 + \mathbf{P}_2^2\right)\right]} \right\} \right] \quad (16)$$

In a practical scenario, residual noise $(\beta)$ due to SIC at the decoding results in ISIC which impacts the performance of the system and it can be modeled as independent and identically distributed (i.i.d) random Gaussian noise with $(0, \sigma^2)$. The corresponding threshold SINR is expressed as,

$$\gamma_{th} = \max\left\{ \frac{\gamma_t(\beta+1)}{\rho\left[\mathbf{P}_k^2 - \gamma_t \mathbf{P}_{\mathcal{K}}^2\right]} \;\;,\;\; \frac{\gamma_t(\beta+1)}{\rho\left[\mathbf{P}_{12}^2 - \gamma_t\left(\mathbf{P}_1^2 + \mathbf{P}_2^2\right)\right]} \right\}. \quad (17)$$

Based on threshold SINR, the closed form outage over the Rayleigh fading channel in presence of ISIC is obtained as,

$$P_{\text{out, ISIC}} = 1 - \exp\left[ -\frac{1}{(\bar{\gamma})^2} \max \left\{ \frac{\gamma_t(\beta+1)}{\rho\left[\mathbf{P}_k^2 - \gamma_t \mathbf{P}_{\mathcal{K}}^2\right]}, \frac{\gamma_t(\beta+1)}{\rho\left[\mathbf{P}_{12}^2 - \gamma_t\left(\mathbf{P}_1^2 + \mathbf{P}_2^2\right)\right]} \right\} \right]. \quad (18)$$

Similar to ISIC, channel estimation error (CEE) is also modeled as an i.i.d random Gaussian noise with $(0, \sigma^2)$ which contributes to ICSI $(K_v)$. CEE impacts the performance of the system and its corresponding threshold SINR is mathematically written as,

$$\gamma_{th} = \max\left\{ \frac{\gamma_t}{\rho\left[\mathbf{P}_k^2 - \gamma_t\left((\mathbf{P}_{\mathcal{K}})^2 + (K_v)^2\right)\right]}, \frac{\gamma_t}{\rho\left[\mathbf{P}_{12}^2 - \gamma_t\left(\mathbf{P}_1^2 + \mathbf{P}_2^2 + (K_v)^2\right)\right]} \right\}. \quad (19)$$

Thus, the closed form OP for the RSMA-based VLC system over the Rayleigh fading channel with ICSI is obtained as,

$$P_{\text{out, ICSI}} = 1 - \exp\left[ -\frac{1}{(\bar{\gamma})^2} \max\left\{ \frac{\gamma_t}{\rho\left[\mathbf{P}_k^2 - \gamma_t\left((\mathbf{P}_{\mathcal{K}})^2 + (K_v)^2\right)\right]}, \frac{\gamma_t}{\rho\left[\mathbf{P}_{12}^2 - \gamma_t\left(\mathbf{P}_1^2 + \mathbf{P}_2^2 + (K_v)^2\right)\right]} \right\} \right]. \quad (20)$$

Furthermore, the closed form outage expression with ISIC and ICSI is obtained by combining (18) and (20) which is expressed as,

$$P_{\text{out, ICSI, ISIC}} = 1 - \exp\left[ -\frac{1}{(\bar{\gamma})^2} \max\left\{ \frac{\gamma_t(\beta+1)}{\rho\left[\mathbf{P}_k^2 - \gamma_t\left((\mathbf{P}_{\mathcal{K}})^2 + (K_v)^2\right)\right]}, \frac{\gamma_t(\beta+1)}{\rho\left[\mathbf{P}_{12}^2 - \gamma_t\left(\mathbf{P}_1^2 + \mathbf{P}_2^2 + (K_v)^2\right)\right]} \right\} \right]. \quad (21)$$

## IV. Outage Analyses Over Rician Fading Channel

In this section, RSMA-based VLC system is analyzed over Rician distribution for indoor environments with relatively unobstructed paths between the transmitter and receiver (there may exist a dominant LOS component). This LOS component can result from direct transmission without significant reflection or scattering which offers more accurate representation of channel conditions for system design and performance analysis [35]. The Rician PDF can be expressed as,

$$P_{\gamma}^{(\gamma)} = \left(\frac{1+K}{\bar{\gamma}}\right) e^{-k-\left(\frac{1+K}{\bar{\gamma}}\right)\gamma} I_0\left(2\sqrt{\frac{K(1+K)\gamma}{\bar{\gamma}}}\right); \gamma \geq 0, \quad (22)$$

where $K$ is the Rician/Rice factor. The outage for the common part is obtained by integrating the threshold SINR in (10) over (22) and expressed as,

$$P_{\text{out, common}} = 1 - \int_{\gamma_{th}}^{\infty} \left(\frac{1+K}{\bar{\gamma}}\right) e^{-K-\left(\frac{1+K}{\bar{\gamma}}\right)\gamma} I_0\left(2\sqrt{\frac{K\left(1+K\right)\gamma}{\bar{\gamma}}}\right) d\gamma. \quad (23)$$

Let the term $\frac{(1+k)\gamma}{\bar{\gamma}}$ in (23) be $\frac{\psi^2}{2}$ such that $d\gamma = \frac{2\psi\gamma}{1+K}.\, d\psi$, the expression of outage is given by,

$$P_{\text{out, common}} = 1 - e^{-k} \int_{\sqrt{2.\gamma_{th}.\frac{1+k}{\bar{\gamma}}.}}^{\infty} \psi e^{-\frac{\psi^2}{2}} I_0\left(\sqrt{2k}\psi\right) d\psi. \quad (24)$$

Simplifying with Yacoub's integral [36], [37] and rearranging (24), the closed form outage expression is obtained as,

$$P_{\text{out, common}} = 1 - Y_{\frac{1}{2}}\left(2\sqrt{K}, \sqrt{\frac{1+K}{\bar{\gamma}}\frac{\gamma_t}{\rho[\mathbf{P}_{12}^2 - \gamma_t(\mathbf{P}_1^2 + \mathbf{P}_2^2)]}}\right). \quad (25)$$

where Yacoub's integral is defined as $Y_{\delta}(\alpha, \beta) = \frac{\sqrt{\pi}\left(1-\alpha^2\right)2^{\left(\frac{3}{2}\right)-\delta}}{\Gamma(\delta)H^{\delta-0.5}\alpha^{-\delta+0.5}} \int_{\beta}^{\infty} \varsigma^{2\mu} e^{-\varsigma^2} I_{\delta-0.5}\left(\alpha^2\varsigma\right) d\varsigma$. Similarly, the outage for the private part is derived for threshold condition and SINR in (14) and (15), respectively. The closed form expression over the Rician PDF is expressed as in (26). Moreover, the overall system is analyzed with residual noise, which is modeled as an i.i.d random Gaussian noise with $(0, \sigma^2)$ for practical suitability, and its corresponding closed-form expression is obtained as in (27).

TABLE I
VLC CHANNEL MODELING PARAMETERS

| Parameters | Values |
|---|---|
| Field of View (FOV) | 60° |
| Incident ($\varpi$) and Radiation angle ($\theta$) | 0°and 30° |
| Optical concentrator gain $g(\varpi)$ | 1 |
| Refractive index ($n$) | 1.5 |
| Detection area of PD ($A_k$) | 1 cm$^2$ |
| Optical filter gain ($\tau(\varpi)$) | 1 |
| Euclidean distance of PD ($d_k$) | 1m |
| PD responsivity ($\zeta$) | 0.4 A/W |
| Lambertian emission order ($m$) | 1 |
| DC bias offset $I_{DC}$ | 700 mA |
| Minimum DC offset $I_L$ | 600 mA |
| Maximum DC offset $I_H$ | 800 mA |

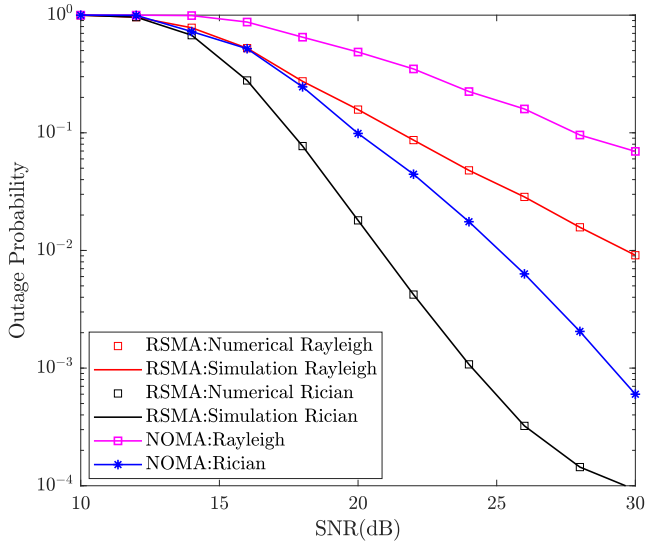


Fig. 3. OP comparison of RSMA and NOMA-based VLC over Rayleigh and Rician fading channels

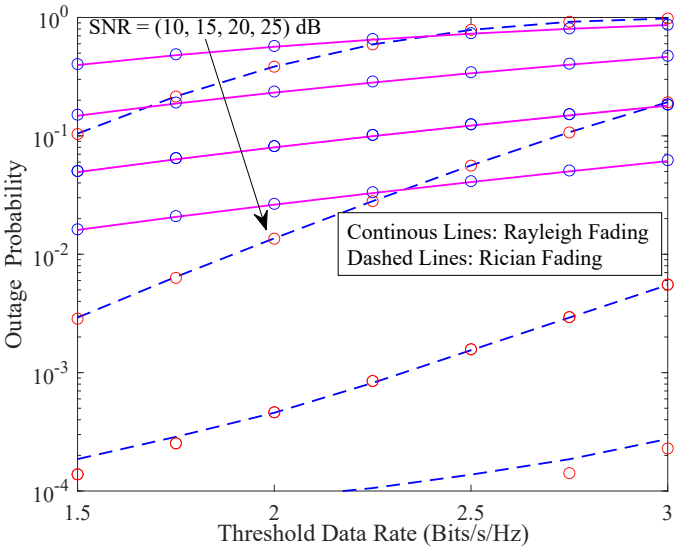


Fig. 4. OP of RSMA-based VLC for various threshold rates

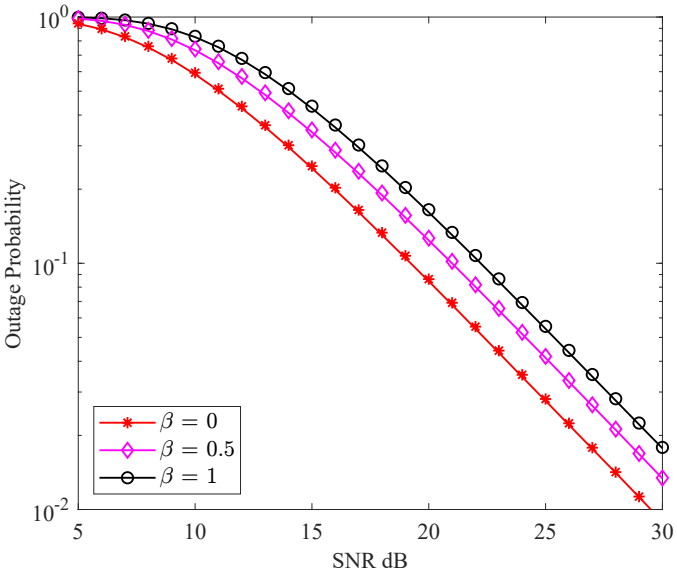


Fig. 5. OP of Rayleigh channel with various residual noise

Now, the CEE is accounted for the outage analysis over the Rician distribution which is also modeled as i.i.d and its closed-form is mathematically realized as in (28). Also, the combined effect of CEE and residual noise can be analyzed for studying the system vulnerability towards outage and its final expression can be obtained as in (29). [Refer Appendix for equations (26)-(29)]. From the obtained final expressions of outage for the common part and private part, analyses with various key parameters are performed for RSMA-based VLC system under the impact of ICSI and ISIC in the upcoming section.

## V. RESULTS AND DISCUSSIONS

In this section, the analytical expressions of OP for downlink RSMA scenario aided through VLC is validated through MC simulation in MATLAB R2021b version for $10^6$ iterations. An analysis is performed with both perfect and imperfect CSI and SIC over Rayleigh and Rician PDF, respectively. Also, the outage performance is analyzed for various threshold values with fixed transmit SNR. The power allocated for the common, private user 1, and private user 2 parts are $0.4$, $0.3$ and $0.3$ respectively, with the threshold data rate of 2 $bits/s/Hz$. The parameters considered for VLC channel coefficient generation modeled through Lambertian emission to simulate the RSMA-based VLC system are listed in Table 1. Fig. 3 traces the OP of RSMA-based VLC system with transmit SNR varying from 10 to 30 $dB$ for Rayleigh and Rician fading channels. Inference shows that as SNR approaches higher values, the system is less outage for both the fading channels due to high signal power. Since the Rician channel considers only LOS path and VLC scenario is aided, its performance is better compared to Rayleigh which accounts for LOS and NLOS paths. Furthermore, it is observed that an average of 10 $dB$ gain is achieved with the Rician channel at a high SNR regime in the VLC-based communication.The analytical closed form expressions derived for OP are validated through MC simulation. Also, the OP of NOMA-based VLC system

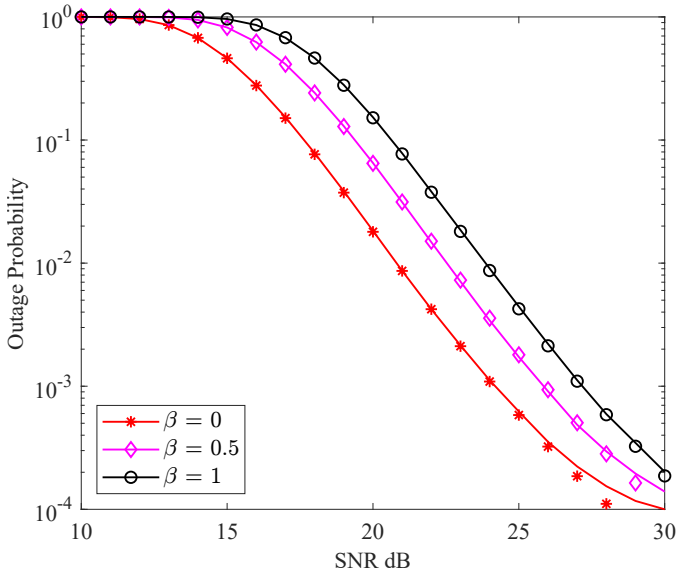


Fig. 6. OP of Rician channel with various residual noise

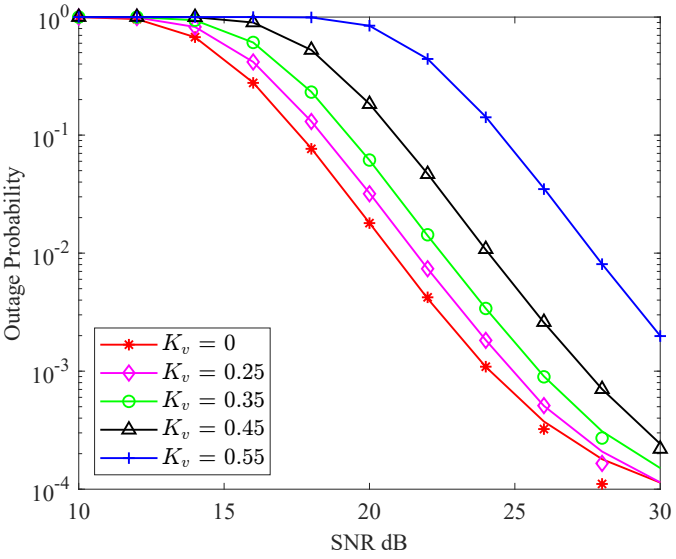


Fig. 8. OP for various ICSI over Rician fading channel

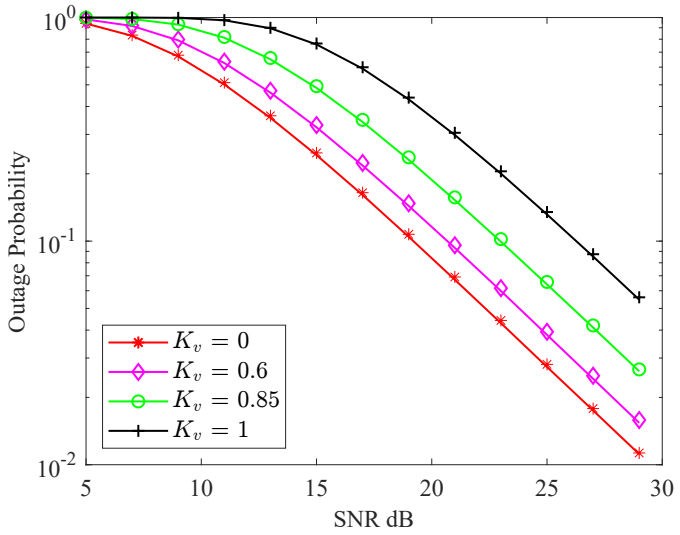


Fig. 7. OP for various ICSI over Rayleigh fading channel

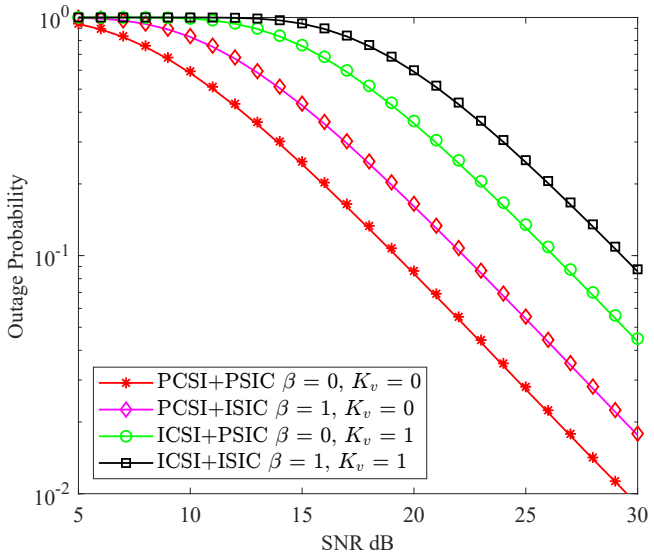


Fig. 9. OP for various ICSI and ISIC over Rayleigh channel

is traced out and contrast with RSMA which shows that a substantial gain is achieved by RSMA over the NOMA. For an outage of $10^{-2}$, the RSMA system achieves a gain of 2 $dB$ and 4 $dB$ for Rayleigh and Rician fading channels respectively over the NOMA system. The effect on OP with varying threshold data rates for specific SNR values $(10, 15, 20, 25)$ $dB$ over Rayleigh and Rician fading channels is shown in Fig. 4. At a high SNR regime, it is perceptible that OP is more in Rayleigh channel and comparatively performs inferior to Rician fading channel due to dominant LOS path. Moreover, as the threshold rate increases, the system outage increases because the reliability decreases for any fixed transmit SNR. Thus, optimal selection of threshold rate is necessary to make the system less outage.

Outage analysis of RSMA-based VLC system with various residual noise $(\beta = 0,\ 0.5,\ 1)$ over Rayleigh and Rician channels is performed and results are displayed in Fig. 5 and 6, respectively. An immediate observation is that at a low SNR regime, the system remains outage for both the fading environments as the signal power is weak and as SNR increases, the outage decreases and better performance is noted in the Rician channel. However, as residual noise increases, OP also increases due to the imperfection in SIC which contributes to additional noise at the PD.

Outage performance of the system under ICSI and perfect SIC over Rayleigh and Rician fading channels is depicted in Fig. 7 and Fig. 8 respectively. Inference reveals that as $K_v$ increases, OP increases i.e., system performance gets degraded due to the CEE. Rayleigh fading channel provides high outage when compared to Rician fading channel due to presence of NLOS component. Finally, the performance of the system with ICSI and ISIC over Rayleigh and Rician fading channels is shown in Fig. 9 and Fig. 10 respectively. The residual noise and CEE parameters are varied within

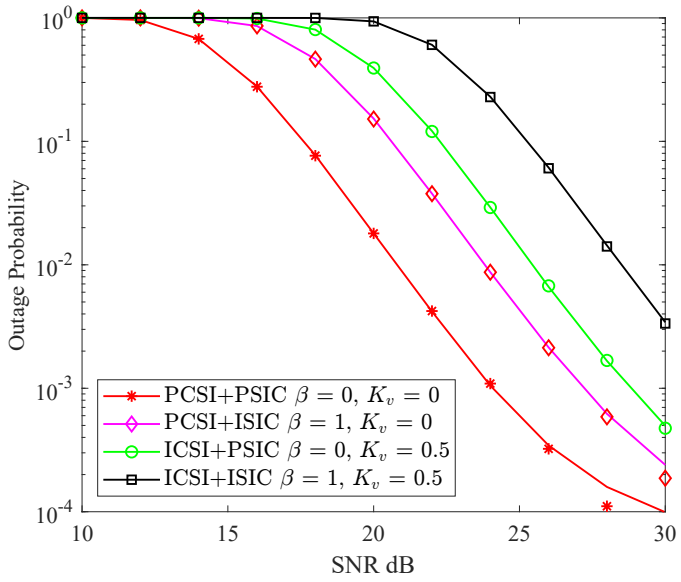


Fig. 10. OP for various ICSI and ISIC over Rician channel

the interval $0 \leq \beta, K_v \leq 1$ for investigation and inferred that OP increases with an increase in $\beta$ and $K_v$ due to additional noise during SIC and error in channel estimated conditions, respectively. Furthermore, it is evident that Rician fading performance is superior to the Rayleigh channel due to the strong LoS component.

## VI. Conclusion

In this paper, an investigation on RSMA-based VLC for downlink scenario is performed. Firstly, we have derived the closed-form OP expressions for Rayleigh and Rician fading channels by considering its corresponding PDF under perfect and imperfect SIC and CSI, respectively. The derived analytical expressions are validated through MC simulations for verifying its correctness. Moreover, the OP analyses is carried out for various key parameters viz., threshold rate, PSIC, PCSI, ISIC and ICSI over Rayleigh and Rician fading channels. From the results of the analyses, it is shown that system outage is less for perfect SIC and CSI values in both the fading channels due to the absence of CEE and residual noise. Furthermore, it is evident that the QoS of RSMA-based VLC system improves with Rician channel due to the LOS component and more outage is observed in the Rayleigh fading channel. Also, the RSMA-based VLC system is compared with NOMA in terms of outage which enacts that RSMA outperforms NOMA-based VLC system. Thus, RSMA-based VLC system aids for indoor communication with enhanced QoS paving the way to 5GB applications with wider bandwidth and unlicensed spectrum. Extension to this work can be optimizing the VLC parameters viz., Lambertian emission order, the optical concentrator gain, detection area of the PD and the optical filter gain for modeling the channel in indoor environment, thereby enhancing the QoS.

## References

[1] O. Dizdar, Y. Mao, W. Han, and B. Clerckx, "Rate-Splitting Multiple Access: A New Frontier for the PHY Layer of 6G," in *2020 IEEE 92nd Vehicular Technology Conference (VTC2020-Fall)*, 2020, pp. 1–7.

[2] M. Rasti, S. K. Taskou, H. Tabassum, and E. Hossain, "Evolution Toward 6G Multi-Band Wireless Networks: A Resource Management Perspective," *IEEE Wireless Communications*, vol. 29, no. 4, pp. 118–125, 2022.

[3] M. Alsabah, M. A. Naser, B. M. Mahmmod, S. H. Abdulhussain, M. R. Eissa, A. Al-Baidhani, N. K. Noordin, S. M. Sait, K. A. Al-Utaibi, and F. Hashim, "6G Wireless Communications Networks: A Comprehensive Survey," *IEEE Access*, vol. 9, pp. 148 191–148 243, 2021.

[4] A. Aldalbahi, "Simulation, performance and interference analysis of multi-user visible light communication systems," 2017.

[5] A. Ndjiongue, H. Ferreira, and T. Ngatched, "Visible light communications (VLC) technology," *Wiley Encyclopedia of Electrical and Electronics Engineering*, 2000.

[6] I. Stefan, H. Burchardt, and H. Haas, "Area spectral efficiency performance comparison between VLC and RF femtocell networks," in *2013 IEEE International Conference on Communications (ICC)*, 2013, pp. 3825–3829.

[7] T. Komine and M. Nakagawa, "Fundamental analysis for visible-light communication system using LED lights," *IEEE Transactions on Consumer Electronics*, vol. 50, no. 1, pp. 100–107, 2004.

[8] A. R. Ndjiongue and K. Ouahada, "Capacity of Outdoor VLC Links Using a Visible LASER Beam," in *2019 International Symposium on Networks, Computers and Communications (ISNCC)*, 2019, pp. 1–6.

[9] P. P. Játiva, C. A. Azurdia-Meza, M. R. Cañizares, S. Céspedes, and S. Montejo-Sánchez, "Performance Enhancement of VLC-Based Systems Using Diversity Combining Schemes in the Receiver," in *2019 IEEE Latin-American Conference on Communications (LATINCOM)*, 2019, pp. 1–6.

[10] S. Ariyanti and M. Suryanegara, "Visible Light Communication (VLC) for 6G Technology: The Potency and Research Challenges," in *2020 Fourth World Conference on Smart Trends in Systems, Security and Sustainability (WorldS4)*, 2020, pp. 490–493.

[11] K. Joshi, N. Roy, G. Singh, V. A. Bohara, and A. Srivastava, "Experimental observations on the feasibility of vlc-based v2x communications under various environmental deterrents," in *2019 IEEE International Conference on Advanced Networks and Telecommunications Systems (ANTS)*, 2019, pp. 1–4.

[12] M. Meucci, M. Seminara, T. Nawaz, S. Caputo, L. Mucchi, and J. Catani, "Bidirectional Vehicle-to-Vehicle Communication System Based on VLC: Outdoor Tests and Performance Analysis," *IEEE Transactions on Intelligent Transportation Systems*, vol. 23, no. 8, pp. 11 465–11 475, 2022.

[13] D. N. Anwar, A. Srivastava, and V. A. Bohara, "Adaptive Channel Estimation in VLC for Dynamic Indoor Environment," in *2019 21st International Conference on Transparent Optical Networks (ICTON)*, 2019, pp. 1–5.

[14] R. Raj, K. Jindal, and A. Dixit, "Fairness Enhancement of Non-Orthogonal Multiple Access in VLC-Based IoT Networks for Intravehicular Applications," *IEEE Transactions on Vehicular Technology*, vol. 71, no. 7, pp. 7414–7427, 2022.

[15] Y. Cheng, T. Zhou, P. Liang *et al.*, "The Improved Precoding Method in the VLC-Based Intelligent Transportation System," *Journal of Advanced Transportation*, vol. 2022, 2022.

[16] M. Zhu, Y. Wang, X. Liu, S. Ma, X. Zhang, and Y. Fu, "Performance Analysis for DF Relay-Aided Visible Light Communication System With NOMA," *IEEE Photonics Journal*, vol. 14, no. 5, pp. 1–9, 2022.

[17] S. Ghosh, "Outage analysis of hybrid VLC–RF system for IoT application under energy harvesting," *Telecommunication Systems*, vol. 84, no. 3, pp. 387–397, 2023.

[18] M. Petkovic, A. Cvetkovic, and M. Narandzic, "Outage Probability Analysis of RF/FSO-VLC Communication Relaying System," in *2018 11th International Symposium on Communication Systems, Networks & Digital Signal Processing (CSNDSP)*, 2018, pp. 1–5.

[19] Y. Mao, B. Clerckx, and V. O. Li, "Energy Efficiency of Rate-Splitting Multiple Access, and Performance Benefits over SDMA and NOMA," in *2018 15th International Symposium on Wireless Communication Systems (ISWCS)*, 2018, pp. 1–5.

[20] Z. Li, C. Ye, Y. Cui, S. Yang, and S. Shamai, "Rate Splitting for Multi-Antenna Downlink: Precoder Design and Practical Implementation," *IEEE Journal on Selected Areas in Communications*, vol. 38, no. 8, pp. 1910–1924, 2020.

[21] S. A. Tegos, P. D. Diamantoulakis, and G. K. Karagiannidis, "On the Performance of Uplink Rate-Splitting Multiple Access," *IEEE Communications Letters*, vol. 26, no. 3, pp. 523–527, 2022.

[22] H. Lei, S. Zhou, K.-H. Park, I. S. Ansari, H. Tang, and M.-S. Alouini, "Outage Analysis of Millimeter Wave RSMA Systems," *IEEE Transactions on Communications*, vol. 71, no. 3, pp. 1504–1520, 2023.

## APPENDIX

$$P_{\text{out, private}} = 1 - Y_{\frac{1}{2}}\left(\sqrt{\frac{1+K}{\bar{\gamma}}\max\left\{\frac{\gamma_t}{\rho\left[\mathbf{P}_k^2 - \gamma_t\mathbf{P}_{\mathcal{K}}^2\right]}, \frac{\gamma_t}{\rho\left[\mathbf{P}_{12}^2 - \gamma_t\left(\mathbf{P}_1^2 + \mathbf{P}_2^2\right)\right]}\right\}}\right) \tag{26}$$

$$P_{out,\ ISIC} = 1 - Y_{\frac{1}{2}}\left(2\sqrt{K}, \sqrt{\frac{1+K}{\bar{\gamma}}\ max\left\{\frac{\gamma_t(\beta+1)}{\rho\left[\mathbf{P}_k^2 - \gamma_t\mathbf{P}_{\mathcal{K}}^2\right]}\ ,\ \frac{\gamma_t(\beta+1)}{\rho\left[\mathbf{P}_{12}^2 - \gamma_t\left(\mathbf{P}_1^2 + \mathbf{P}_2^2\right)\right]}\right\}}\right). \tag{27}$$

$$P_{out,ICSI} = 1 - Y_{\frac{1}{2}}\left(2\sqrt{K}, \sqrt{\frac{1+K}{\bar{\gamma}}\ max\left\{\frac{\gamma_t}{\rho\left[\mathbf{P}_k^2 - \gamma_t\ \left(\left(\mathbf{P}_{\mathcal{K}}\right)^2 + \left(K_v\right)^2\right)\right]}\ ,\ \frac{\gamma_t}{\rho\left[\mathbf{P}_{12}^2 - \gamma_t\left(\mathbf{P}_1^2 + \mathbf{P}_2^2 + \left(K_v\right)^2\right)\right]}\right\}}\right). \tag{28}$$

$$P_{out,ICSI,ISIC} = 1 - Y_{\frac{1}{2}}\left(2\sqrt{K}, \sqrt{\frac{1+K}{\bar{\gamma}}max\left\{\frac{\gamma_t\left(\beta+1\right)}{\rho\left[\mathbf{P}_k^2 - \gamma_t\left(\left(\mathbf{P}_{\mathcal{K}}\right)^2 + \left(K_v\right)^2\right)\ \right]}, \frac{\gamma_t\left(\beta+1\right)}{\rho\left[\mathbf{P}_{12}^2 - \gamma_t\left(\mathbf{P}_1^2 + \mathbf{P}_2^2 + \left(K_v\right)^2\right)\right]}\right\}}\right). \tag{29}$$


[23] X. Gao, X. Li, C. Han, M. Zeng, H. Liu, S. Mumtaz, and A. Nallanathan, "Rate-Splitting Multiple Access-based Cognitive Radio Network With ipSIC and CEEs," 2022.

[24] F. Xiao, X. Li, L. Yang, H. Liu, and T. A. Tsiftsis, "Outage Performance Analysis of RSMA-Aided Semi-Grant-Free Transmission Systems," *IEEE Open Journal of the Communications Society*, vol. 4, pp. 253–268, 2023.

[25] C. Hao and B. Clerckx, "MISO Networks With Imperfect CSIT: A Topological Rate-Splitting Approach," *IEEE Transactions on Communications*, vol. 65, no. 5, pp. 2164–2179, 2017.

[26] S. Naser, P. C. Sofotasios, L. Bariah, W. Jaafar, S. Muhaidat, M. Al-Qutayri, and O. A. Dobre, "Rate-Splitting Multiple Access: Unifying NOMA and SDMA in MISO VLC Channels," *IEEE Open Journal of Vehicular Technology*, vol. 1, pp. 393–413, 2020.

[27] S. Tao, H. Yu, Q. Li, Y. Tang, and D. Zhang, "One-Layer Rate-Splitting Multiple Access Benefits over Power-Domain NOMA in Indoor Multi-Cell Visible Light Communication Networks," in *2020 IEEE International Conference on Communications Workshops (ICC Workshops)*, 2020, pp. 1–7.

[28] F. Xing, S. He, V. C. M. Leung, and H. Yin, "Energy Efficiency Optimization for Rate-Splitting Multiple Access-Based Indoor Visible Light Communication Networks," *IEEE Journal on Selected Areas in Communications*, vol. 40, no. 5, pp. 1706–1720, 2022.

[29] S. A. Naser, P. C. Sofotasios, S. Muhaidat, and M. Al-Qutayri, "Rate-Splitting Multiple Access for Indoor Visible Light Communication Networks," in *2021 IEEE Wireless Communications and Networking Conference Workshops (WCNCW)*, 2021, pp. 1–7.

[30] S. Ma, H. Zhou, Y. Mao, X. Liu, Y. Wu, B. Clerckx, Y. Wang, and S. Li, "Robust beamforming design for rate splitting multiple access-aided MISO visible light communications," *arXiv preprint arXiv:2108.07014*, 2021.

[31] M. Zhu, Y. Wang, X. Liu, S. Ma, X. Zhang, and Y. Fu, "Performance Analysis for DF Relay-Aided Visible Light Communication System With NOMA," *IEEE Photonics Journal*, vol. 14, no. 5, pp. 1–9, 2022.

[32] K. Srinivasarao and M. Surendar, "Outage Analysis of Downlink Non-Orthogonal Multiple Access Scheme Over Rician Fading Channel," in *2020 IEEE 4th Conference on Information & Communication Technology (CICT)*, 2020, pp. 1–5.

[33] H. S. Khallaf, A. S. Ghazy, H. M. H. Shalaby, and S. S. A. Obayya, "Performance analysis of visible light communication systems over fading channels," in *2017 19th International Conference on Transparent Optical Networks (ICTON)*, 2017, pp. 1–4.

[34] F. Miramirkhani and M. Uysal, "Channel modelling for indoor visible light communications," *Philosophical Transactions of the Royal Society A*, vol. 378, no. 2169, p. 20190187, 2020.

[35] A. R. Ndjiongue, T. M. N. Ngatched, and H. C. Ferreira, "On the Indoor VLC Link Evaluation Based on the Rician $K$ -Factor," *IEEE Communications Letters*, vol. 22, no. 11, pp. 2254–2257, 2018.

[36] A. Prudnikov, *Integrals and series: direct Laplace transforms*.

[37] R. Courant, *Differential and Integral Calculus*. John Wiley & Sons, 2011, vol. 2.



**Sundaresan Sabapathy (Graduate Student Member, IEEE)** received his B.Tech(ECE) degree from Pondicherry University, Puducherry and M.Tech degree in Remote Sensing and Wireless Sensor Networks from Amrita Vishwa Vidyapeetham, Coimbatore. He has 5 years of teaching experience and have published around 25 research articles and book chapters in various reputed journals and international conferences. He is currently pursuing his Ph.D. in Wireless communications from National Institute of Technology, Puducherry. His research interests are URLLC, Next generation multiple access, PHY Layer design, 5G and Beyond systems.



**Surendar Maruthu (Member, IEEE)** is an Assistant Professor in the Department of Electronics and communication engineering at NIT Puducherry. He did his B.E.(ECE) and M.Tech. (ECE) from Thiagarajar College of Engineering, Madurai, and Ph.D. (ECE) from National Institute of Technology, Thiruchirapalli. He has published several research articles in various reputed journals and international conferences. He delivered several guest lectures and key note speech in various premier institutes. Since 2018, he has been an Assistant Professor with the Department of Electronics and Communication Engineering, National Institute of Technology Puducherry, Puducherry, India. He is co-principal investigator for the project from Sri Lanka Technological Campus (SLTC), Srilanka. His research interests include PHY layer prospective of 5G and Beyond Wireless Communication, Signal Processing, etc.